Current Research in Pharmacology and Drug Discovery 2 (2021) 100061

Contents lists available at ScienceDirect

Current Research in Pharmacology and Drug Discovery

journal homepage: www.journals.elsevier.com/current-research-in-pharmacology-and-drug-discovery

SENP2 is vital for optimal insulin signaling and insulin-stimulated glycogen synthesis in human skeletal muscle cells

Jenny Lund [a,*,1], Solveig A. Krapf [a,1], Medina Sistek [a], Hege G. Bakke [a], Stefano Bartesaghi [b], Xiao-Rong Peng [b], Arild C. Rustan [a], G. Hege Thoresen [a,c], Eili T. Kase [a]

[a] Section for Pharmacology and Pharmaceutical Biosciences, Department of Pharmacy, University of Oslo, Norway
[b] Bioscience Metabolism, Research and Early Development, Cardiovascular, Renal and Metabolism (CVRM) BioPharmaceuticals R&D, AstraZeneca, Gothenburg, Sweden
[c] Department of Pharmacology, Institute of Clinical Medicine, University of Oslo, Norway

ARTICLE INFO

Keywords:
SENP2
Lentivirus
Knockdown
Primary human myotubes
Energy metabolism
Insulin sensitivity

ABSTRACT

Sentrin-specific protease (SENP) 2 has been suggested as a possible novel drug target for the treatment of obesity and type 2 diabetes mellitus after observations of a palmitate-induced increase in SENP2 that lead to increased fatty acid oxidation and improved insulin sensitivity in skeletal muscle cells from mice. However, no precedent research has examined the role of SENP2 in human skeletal muscle cells. In the present work, we have investigated the impact of SENP2 on fatty acid and glucose metabolism as well as insulin sensitivity in human skeletal muscle using cultured primary human myotubes. Acute (4 h) oleic acid oxidation was reduced in SENP2-knockdown (SENP2-KD) cells compared to control cells, with no difference in uptake. After prelabeling (24 h) with oleic acid, total lipid content and incorporation into triacylglycerol was decreased, while incorporation into other lipids, as well as complete oxidation and β-oxidation was increased in SENP2-KD cells. Basal glucose uptake (i.e., not under insulin-stimulated conditions) was higher in SENP2-KD cells, whereas oxidation was similar to control myotubes. Further, basal glycogen synthesis was not different in SENP2-KD myotubes, but both insulin-stimulated glycogen synthesis and Akt^{Ser473} phosphorylation was completely blunted in SENP2-KD cells. In conclusion, SENP2 plays an important role in fatty acid and glucose metabolism in human myotubes. Interestingly, it also appears to have a pivotal role in regulating myotube insulin sensitivity. Future studies should examine the role of SENP2 in regulation of insulin sensitivity in other tissues and *in vivo*, defining the potential for SENP2 as a drug target.

1. Introduction

Type 2 diabetes mellitus (T2DM) is a significant contributor to morbidity and mortality in the population worldwide. T2DM develops due to insulin resistance and is characterized by impaired insulin-dependent glucose metabolism in metabolic important tissues, such as skeletal muscles, liver and adipose tissue (reviewed in (Czech, 2017)). Obesity is a strong risk factor for development of insulin resistance. Under circumstances where access to fatty acids exceeds oxidative capacity, as typically seen in obesity, lipid accumulates in other organs than adipose tissue (Boren et al., 2013). Thus, increasing fatty acid oxidation and/or decreasing lipid storage in skeletal muscles can reverse such insulin resistance (Perdomo et al., 2004; Choi et al., 2007; Feige et al., 2008; Bruce et al., 2009). Ectopic storage of fatty acids (mainly triacylglycerols (TAG)) correlates with decreased insulin sensitivity (reviewed in (Kelley and Goodpaster, 2001)). This can change insulin-signaling pathways and reduce insulin-stimulated uptake of glucose (Sugden and Holness, 2006; Holloway, 2009). Skeletal muscle cells from individuals with T2DM have shown a reduced ability to oxidize fatty acids, an increased storage of intracellular lipids, reduced insulin-stimulated glycogen synthesis and reduced Akt phosphorylation (Gaster et al., 2004; Kase et al. 2005, 2015; Corpeleijn et al., 2010).

The mechanisms underlying insulin resistance are not fully elucidated; however, increased levels of plasma free fatty acids and TAG, as well as hyperglycemia are suggested as causal factors (Tomás et al., 2002; Aas et al. 2004, 2005, 2006, 2011; Petersen and Shulman, 2006).

* Corresponding author. Section for Pharmacology and Pharmaceutical Biosciences, Department of Pharmacy, University of Oslo, P.O. Box 1068 Blindern, 0316 Oslo, Norway.
E-mail address: jenny.lund@farmasi.uio.no (J. Lund).
[1] Shared first authorship.

https://doi.org/10.1016/j.crphar.2021.100061
Received 18 June 2021; Received in revised form 15 September 2021; Accepted 23 September 2021

Moreover, abnormal lipid metabolism with accumulation of lipotoxic intermediates (including DAG) and TAG and mitochondrial dysfunction in skeletal muscle have been linked to insulin resistance and development of T2DM (Martins et al., 2012). Furthermore, intracellular localization affects how these lipids affect muscle insulin sensitivity (Perreault et al., 2018). Blunted effects of insulin on insulin-dependent glucose uptake and changed insulin signaling has previously been reported in myotubes from individuals with T2DM (Kase et al., 2015). The insulin resistance in myotubes is thought to be caused by defects in the insulin signal transduction cascade: insulin receptor, insulin receptor substrate 1, phosphoinositide 3-kinase, and Akt activity (Petersen and Shulman, 2018).

Peroxisome proliferator-activated receptors (PPARs) are members of a nuclear receptor family known to serve key roles in regulation of energy metabolism in important metabolic organs (skeletal muscle, adipose tissue and liver). PPARγ is mainly expressed in adipose tissue, but also found in muscle and liver, and has an important role in lipid metabolism and increasing insulin sensitivity in these tissues (Desvergne and Wahli, 1999). However, PPARδ is the main subtype in skeletal muscle (Desvergne and Wahli, 1999). PPARs are known targets for SUMOylation (SUMO = small ubiquitin-related modifier) (Yamashita et al., 2004; Rytinki and Palvimo, 2009; Do Koo et al., 2015), a post-translational protein modification system with reversible activity (Hay, 2005). SUMOylation has an inhibitory effect on PPARγ and PPARδ translational activity and consequently for their target genes (Chung et al., 2010; Do Koo et al., 2015). SUMOylated PPARs are activated when deSUMOylated by a SUMO specific protease (SENP) (Huang et al., 2009). The SENPs are a family of cysteine proteases that deSUMOylates different target proteins (Nayak and Müller, 2014). SENP2 plays an important role in numerous processes in the body by maturing and deSUMOylating SUMOs (Reverter and Lima, 2006; Mikolajczyk et al., 2007; Békés et al., 2011). It has been shown in mice cells (C2C12 myotubes and 3T3-L1 preadipocytes) that SENP2 increases the activity of PPARδ and PPARγ by deSUMOylation (Chung et al., 2011; Do Koo et al., 2015). Further, studies have shown that SENP2 is induced by leptin and that it is an important regulator of fatty acid metabolism in skeletal muscle of mice (Do Koo et al. 2015, 2019).

The role of SENP2 in human skeletal muscle has not previously been explored. However, studies in mice have suggested a regulatory role on fatty acid metabolism in skeletal muscle (Do Koo et al., 2015). In addition, as SENP2s role in skeletal muscle glucose metabolism and insulin resistance has not yet been explored. The main purpose of this study was to elucidate how knockdown of SENP2 (SENP2-KD) in human skeletal muscle cells would influence basal (i.e., not insulin-stimulated) lipid and glucose metabolism. Further, we wanted to examine how SENP2-KD affected insulin sensitivity as measured by insulin response on glycogen synthesis and Akt phosphorylation.

2. Materials and methods

2.1. Materials

Corning® CellBIND® tissue culture plates were from Corning (Schiphol-Rijk, the Netherlands). Nunc™ Cell Culture Treated Flasks with Filter Caps, Nunc™ 96-MicroWell™ plates, DMEM-Glutamax™ low glucose with sodium pyruvate, human epidermal growth factor (hEGF), PBS, FBS, trypsin-EDTA, Pierce™ BCA Protein Assay Kit, Super Signal™ West Femto Maximum Sensitivity substrate, GeneJET Plasmid Maxiprep Kit, High-Capacity cDNA Reverse Transcription Kit, TaqMan reverse transcription kit reagents, MicroAmp® Optical 96-well Reaction Plate, MicroAmp® Optical Adhesive Film, Power SYBR® Green PCR Master Mix, and primers for TaqMan PCR were from Thermo Fisher Scientific (Waltham, MA, US). Insulin (Actrapid® Penfill® 100 IE/ml) was from Novo Nordisk (Bagsvaerd, Denmark). PromoCell®, dexamethasone, HEPES, 2-[2-[4-(trifluoromethoxy)phenyl]hydrazinylidene]-propanedinitrile (FCCP), D-glucose, oleic acid (18:1, n-9), BSA (essentially fatty acid-free), L-carnitine, glycogen (bovine), perchloric acid, β-mercaptoethanol, phosphatase inhibitor, and protease inhibitor were from Sigma-Aldrich (St. Louis, MO, US). RNeasy Mini Kit was from QIAGEN (Venlo, the Netherlands). D-[^{14}C(U)]glucose (111 and 10175 MBq/mmol) and [1-^{14}C]oleic acid (2183 MBq/mmol) were from PerkinElmer NEN® (Boston, MA, US). Ultima Gold™ XR, Pico Prias 6 ml PE vials, 96-well Isoplate®, Unifilter®-96 GF/B, and TopSeal®-A transparent film were from PerkinElmer (Shelton, CT, US). Tris-HCl, glycerol and thin layer chromatography (TLC) silica gel 60 plates were from Merck (Darmstadt, Germany). Free fatty acids (FFA, 2 mg/ml), cholesterol ester (CE, 2 mg/ml) and mono-, di-, triglyceride mix (4 mg/ml) were from Supelco (Bellefonte, PA, US). Bio-Rad Protein Assay Dye Reagent Concentrate, Bio-Rad Precision Plus Protein™ Dual Color standard, bromophenol blue, Trans-Blot® Turbo™ Mini-size Transfer nitrocellulose membranes, Trans-Blot® Turbo™ Mini-size Transfer Stacks, Clarity Western ECL substrates, Tris/glycine/SDS buffer, and Tween 20 were from Bio-Rad (Copenhagen, Denmark). Anti-rabbit and anti-mouse IgG (HRP linked) antibodies, antibodies against myosin heavy chain (MHC) IIa (3403S), β-actin (4970) and α-tubulin (2144), and antibodies against total and phosphorylated Akt at Ser473 (9272 and 9271S, respectively) were from Cell Signaling Technology® Inc. (Beverly, MA, US). Antibody against SENP2 (ab124724) was from Abcam (Cambridge, UK). Antibody against MHCI (MAB1628) was from Millipore (Temecula, MA, US). pMD2.G and psPAX2 were generously provided by Addgene's non-profit repository (Watertown, MA, US) after deposition by Didier Trono on behalf of his lab. GIPZ human shRNA for SENP2-KD (RHS4430-200215 612, clone-ID V2LHS_201 229) and GIPZ shRNA empty vector control (RHS4349) were purchased as glycerol stocks from Horizon Discovery (Cambridge, UK).

2.2. Ethical approvals

Biopsies were obtained after informed written consent and approval by Regional Committees for Medical and Health Research Ethics (REK) North, Tromsø, Norway (ref. no. 2011/882). The study adhered to the Code of Ethics of the World Medical Association (Declaration of Helsinki).

2.3. Production of lentivirus particles

Glycerol stocks were prepared of the pMD2.G envelope plasmid and psPAX2 packaging plasmid. Plasmid DNA was isolated from pMD2.G, psPAX2, SENP2, and SCR shRNAs. Lentivirus particles containing human SENP2 shRNA or control (scrambled (SCR)) shRNA were generated through transient transfection of HEK293T cells as previously described (Barde et al., 2010).

2.4. Transduction of cultured primary human myoblasts

Satellite cells were established from biopsies of *musculus vastus lateralis* and a cell bank was established as described previously (Lund et al., 2017). A mixture of cells from six different donors (in passage 2) was cultured in 75 cm^2 Nunc flasks until 40% confluence. Then, the cells were transduced (MOI = 0.5) with shRNA viral particles targeting SENP2 or control. Polybrene (8 μg/ml) was used as transfection reagent. Transduced cells were selected with puromycin (0.5 μg/ml) 72 h after viral infection and cultured to approximately 90% confluence before frozen down to create a cell bank with transduced myoblasts (passage 3). There were no visual differences to be observed in the microscope after transducing the cells with lentivirus (except the GFP tag). The cells divided as normal and as explained below their differentiation ability was intact. This indicates no loss in cell viability.

2.5. Cell culturing

For proliferation of transduced myoblasts, a DMEM-Glutamax™ (5.5 mmol/l glucose) medium supplemented with 10% FBS, 10 ng/ml

hEGF, 0.39 μg/ml dexamethasone, and 0.05% BSA. At approximately 80% confluence the medium was changed to DMEM-Glutamax™ (5.5 mmol/l glucose) supplemented with 2% FBS and 25 pmol/l insulin to initiate differentiation into multinucleated myotubes. The cells were allowed to differentiate for 7 days. The cells were cultured in a humidified 5% CO_2 atmosphere at 37 °C, and medium was changed every 2-3 days. Experiments were performed on cells from passage 3.

2.6. Acute substrate oxidation assay and measurement of acid-soluble metabolites (ASM)

Skeletal muscle cells (7000 cells/well) were cultured on 96-well CellBIND® microplates. Substrate, D-[^{14}C(U)]glucose (18.5 kBq/ml, 200 μmol/l) or [1-^{14}C]oleic acid (18.5 kBq/ml, 100 μmol/l) was given acutely during 4 h CO_2 trapping as described previously (Wensaas et al., 2007). CO_2 production (complete oxidation) and cell-associated radioactivity (CA) were assessed using a PerkinElmer 2450 MicroBeta^2 scintillation counter (PerkinElmer). Protein content in each well was determined with the Bio-Rad protein assay using a VICTOR™ *X*4 Multilabel Plate Reader (PerkinElmer). Measurement of acid-soluble metabolites (ASM), reflecting incomplete fatty acid oxidation (β-oxidation) and mainly consists of tricarboxylic acid cycle metabolites, was performed as previously described by Skrede et al., (1994) and modified by Bakke et al., (2012). In short, 100 μl of the radiolabeled medium was transferred to an Eppendorf tube and precipitated with 300 μl cold $HClO_4$ (1 mol/l) and 30 μl BSA (6%). Thereafter, the tube was centrifuged at 10 000 rpm/10 min/4 °C before 200 μl of the supernatant was counted by liquid scintillation of a Pacard Tri-Carb 1900 TR (PerkinElmer). The sum of $^{14}CO_2$ and CA was considered as total substrate uptake of glucose, whereas the sum of $^{14}CO_2$, ASM and CA was considered as total substrate uptake of oleic acid.

2.7. Glycogen synthesis

Cells were cultured and differentiated as described in subsection 2.5. Once fully differentiated, myotubes were starved for 1.5 h in glucose-free medium before exposed to serum-free DMEM (5.5 mmol/l glucose) supplemented with D-[^{14}C(U)]glucose (18.5 kBq/ml, 0.67 mmol/l), in absence or presence of 20 nmol/l or 100 nmol/l insulin for 3 h to measure glycogen synthesis. The cells were washed twice with PBS and harvested in 1 mol/l KOH. Protein content was determined by the Pierce BCA Protein Assay Kit before 20 mg/ml glycogen and more KOH (final concentration 4 mol/l) were added to the samples. Then, D-[^{14}C(U)]glucose incorporated into glycogen was measured as previously described (Hessvik et al., 2010).

2.8. Prelabeling with oleic acid to study lipid distribution and oxidation

Myotubes were incubated with [1-^{14}C]oleic acid (18.5 kBq/ml, 100 μM) for the last 24 h of the differentiation period. After prelabeling, parts of the radiolabeled medium were transferred to a 96-well plate (100 μl radiolabeled medium/well) and the rest to Eppendorf tubes and immediately frozen down at −20 °C for later measurement of complete oxidation (CO_2) and ASM, respectively. The cells were then washed twice with PBS and harvested in 250 μl 0.1% SDS. Cellular lipids were isolated as previously described (Gaster et al., 2004) by extraction of the homogenized cell fraction, separation of lipids by thin layer chromatography (TLC) and quantification by liquid scintillation (Tri-Carb, 1900; PerkinElmer). A non-polar solvent mixture of hexane:diethyl ether:acetic acid (65:35:1) was used to separate the lipids. The amount of lipids was related to total cell protein concentration determined by the Pierce protein assay.

For measurement of complete oxidation (CO_2) after prelabeling, 40 μl perchloric acid (1 mol/l) was added to the frozen radiolabeled medium before mounted in the appliance described by Wensaas et al., (2007). ASM after prelabeling with oleic acid was measured as described in subsection 2.6.

2.9. RNA isolation and analysis of gene expression by qPCR

Transduced primary human skeletal muscle cells were cultured in 6-well CellBIND® tissue culture plates as described in subsection 2.5. Total RNA was isolated using QIAGEN RNeasy Mini Kit according to the supplier's protocol. Total RNA was reversely transcribed using a High-Capacity cDNA Reverse Transcription Kit and TaqMan Reverse Transcription Reagents using a PerkinElmer 2720 Thermal Cycler (25 °C for 10 min, 37 °C for 80 min and 85 °C for 5 min). Primers were designed using Primer Express® (Thermo Fisher Scientific). qPCR was performed using a StepOnePlus Real-Time PCR system (Thermo Fisher Scientific). Target genes were quantified in duplicates carried out in a 25 μl reaction volume according to the supplier's protocol. All assays were run for 44 cycles (95 °C for 15 s followed by 60 °C for 60 s). Expression levels were normalized to the housekeeping gene ribosomal protein lateral stalk subunit P0 (*RPLP0*). The housekeeping gene glyceraldehyde 3-phosphate dehydrogenase (*GAPDH*) was also analyzed; there were no differences between normalizing for *RPLP0* or *GAPDH*. Forward and reverse primers were used at a concentration of 30 μmol/l. Primer sequences and accession numbers are presented in Table 1.

2.10. Immunoblotting

Myotubes were harvested in Laemmli buffer (0.5 mol/l Tris-HCl, 10% SDS, 20% glycerol, 10% β-mercaptoethanol, and 5% bromophenol blue). The proteins were electrophoretically separated on 4–20% Mini-Protean TGX™ gels with Tris/glycine buffer (pH 8.3) followed by blotting to nitrocellulose membranes and incubation with antibodies. Immunoreactive bands were visualized with enhanced chemiluminescence (Chemidoc XRS, Bio-Rad) and quantified with Image Lab (version 6.0.1) software. Expression of SENP2 was normalized to expression of the housekeeping protein β-actin. Expressions of MHCI and MHCIIa were normalized to expression of the housekeeping protein α-tubulin. Phosphorylation of Akt at Ser473 was normalized for total Akt expression. Immunoblots with merging of protein of interest with protein standard are presented as supplementary material.

2.11. Presentation of data and statistics

All values are reported as mean ± SEM. The value *n* represents the number of individual experiments, each with at least duplicate measurements. Statistical analyses were performed using GraphPad Prism 8.3.0 for Windows (GraphPad Software Inc., La Jolla, CA, US) and SPSS version 27 (IBM® SPSS® Statistics for Windows, Armonk, NY, US).

Table 1
Description of primers.

Gene	Acc.no.	Forward sequence	Reverse sequence
GAPDH	NM002046	TGC ACC ACC ACC TGC TTA GC	GGC ATG GAC TGT GGT CAT GAG
GLUT1	K03195	CAG CAG CCC TAA GGA TCT CTC A	CCG GCT CGG CTG ACA TC
IRS1	NM_005544.2	CTA CTC AAA AGG GAG CGG AGA TAA	AAT AAC GGA CAC TGC ACA ACA GTC T
MYH2	C5814	AAG GTC GGC AAT GAG TAT GTC A	CAA CCA TCC ACA GGA ACA TCT TC
MYH7	NM_000257.2	CTC TGC ACA GGG AAA ATC TGA A	CCC CTG GAC TTT GTC TCA TT
PDK4	BC040239	TTT CCA GAA CCA ACC AAT TCA CA	TGC CCG CAT TGC ATT CTT A
RPLP0	M17885	CCA TTC TAT CAT CAA CGG GTA CAA	AGC AAG TGG GAA GGT GTA ATC C
SENP2	NM_021627.2	CTG AGG CGT CCC CAT TGT	CTT TCG GTA CTT CTC TCT TTC CTC TT

GAPDH, glyceraldehyde 3-phosphate dehydrogenase; *GLUT1*, glucose transporter 1; *IRS1*, insulin receptor substrate 1; *MYH*, myosin heavy chain; *PDK4*, pyruvate dehydrogenase kinase 4; *RPLP0*, ribosomal protein lateral stalk subunit P0; SENP2, SUMO specific protease 2.

Paired *t*-test or mixed-model analysis was used to evaluate the knockdown effect. Linear mixed-model analysis was used to compare differences between conditions with within-donor variation and simultaneously compare differences between groups with between-donor variation. The linear mixed-model analysis includes all observations in the statistical analyses and takes into account that not all observations are independent. A p value ≤ 0.05 was considered significant.

3. Results

3.1. Gene expression of SENP2 and fiber type markers increase with differentiation

To determine optimal time point for knockdown of the SENP2 gene in primary human skeletal muscle cells, we analyzed mRNA expression of *SENP2* as well as the differentiation markers *MYH7* and *MYH2* at initiation of differentiation (0 h) and thereafter every 2 h for the first 12 h of differentiation, followed by harvesting 1 day after differentiation and every second day until the final seventh day of differentiation. As expected, gene expression of *MYH7* (Fig. 1A), *MYH2* (Fig. 1B) and *SENP2* (Fig. 1C) increased with time of differentiation. Therefore, we decided to transduce the cells while they were myoblasts and then differentiate the transduced cells. SENP2-KD was confirmed by mRNA expression and immunoblotting (Fig. 2A and B/C, respectively). A non-transduced cell sample was also included to ensure that the scrambled virus did not affect the cells; no differences were observed (supplementary material). As SENP2-KD was performed prior to cell differentiation, protein expressions of MHCI and MHCIIa were measured to ensure that the ability of the myoblasts to differentiate into myotubes was not affected by SENP2-KD. Protein expressions of MHCI and MHCIIa were not affected by SENP2-KD (Fig. 3).

3.2. SENP2-KD in human myotubes reduced oxidation and oxidative reserve capacity after acute oleic acid incubation

To examine the role of SENP2 in fatty acid metabolism (Fig. 4), cell-associated oleic acid, complete oleic acid oxidation (CO_2) and acid-soluble metabolites (ASM) reflecting β-oxidation of oleic acid were measured in SENP2-KD myotubes and compared with control myotubes after 4 h. Total uptake and fractional oxidation of oleic acid were also calculated. SENP2-KD resulted in decreased complete oxidation (Fig. 4B) and fractional oxidation (Fig. 4E), i.e., oxidation relative to total uptake of oleic acid, as well as reduced oxidative reserve capacity (Fig. 4F). There were not observed any differences in accumulation (Fig. 4A) and uptake (Fig. 4D) of oleic acid, or incomplete fatty acid β-oxidation (Fig. 4C).

3.3. SENP2-KD in human myotubes reduced oleic acid incorporation into cellular lipids and increased oxidation of prelabeled oleic acid

To further examine changes in oleic acid metabolism we wanted to examine how SENP2-KD affected fatty acid distribution into complex lipids (Fig. 5). The myotubes were prelabeled with oleic acid for 24 h and incorporation into different lipid classes was measured by thin layer chromatography. SENP2-KD reduced the incorporation of oleic acid into total lipids, phospholipids (PL), diacylglycerol (DAG), TAG, and CE, whereas the level of unesterified oleic acid (FFA) was slightly increased (Fig. 5A). When adjusting the results for the much lower oleic acid incorporation in the knockdown cells it was observed that SENP2-KD in fact increased the relative incorporation into all lipid classes except for TAG, which remained reduced (Fig. 5B). In addition, oxidation (CO_2) and β-oxidation (ASM) after prelabelling with oleic acid for 24 h were markedly increased after SENP2-KD in myotubes (Fig. 6A and B, respectively).

3.4. SENP2-KD in human myotubes increased glucose uptake

To examine the role of SENP2 in glucose metabolism (Fig. 7), oxidation and cell-associated glucose were measured in SENP2-KD myotubes and compared with control myotubes. Total uptake and fractional oxidation of glucose were also calculated. SENP2-KD resulted in increased accumulation of glucose as measured by cell-associated radioactivity (Fig. 7A) as well as increased total glucose uptake (Fig. 7C), despite no change in glucose oxidation (Fig. 7B). However, fractional glucose oxidation, i.e., oxidation relative to total glucose uptake, was significantly reduced in SENP2-KD cells (Fig. 7D).

3.5. SENP2-KD in human myotubes blunted insulin-stimulated glycogen synthesis

In order to further analyze the role of SENP2 in glucose metabolism and its role on insulin sensitivity, basal and insulin-stimulated glycogen synthesis were examined (Fig. 8A). Basal glycogen synthesis was not different between control and SENP2-KD myotubes. Treatment with 100 nmol/l insulin increased glycogen synthesis in control myotubes, but not in SENP2-KD myotubes. To examine the mechanism behind this result, the response to 100 nmol/l insulin was evaluated by assessment of Akt phosphorylation at serine 473 (Fig. 8B and C). No changes in the basal level of pAkt/total Akt ratio were observed between cells from control and SENP2-KD. In line with the blunted insulin-stimulated glycogen synthesis, no effect of insulin on pAkt/total Akt ratio were observed in myotubes with downregulated SENP2 expression, whereas the control myotubes showed the expected increased pAkt/total Akt ratio after insulin stimulation (Fig. 8C). However, total Akt protein expression

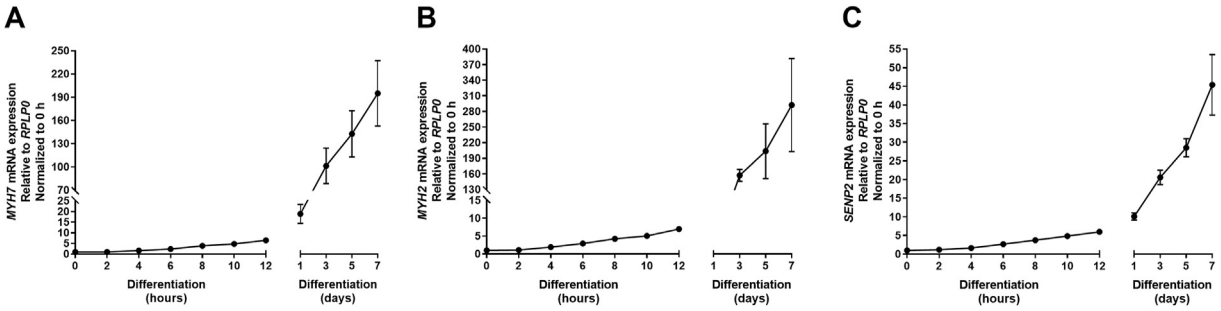

Fig. 1. Gene expression of fiber type markers and SENP2 throughout muscle cell differentiation. Cells were harvested every 2 h for the first 12 h of the differentiation period, then at day 1 of differentiation and every 2 days until day 7 of differentiation. RNA was harvested and expression of myosin heavy chain (*MYH*) *7* (**A**), *MYH2* (**B**) and SUMO specific peptidase (*SENP*) *2* (**C**) was analyzed by qPCR. Results are shown as mean ± SEM relative to the housekeeping gene ribosomal protein lateral stalk subunit P0 (*RPLP0*) and normalized to the time point where differentiation was initiated (0 h), from three individual experiments ($n = 3$).

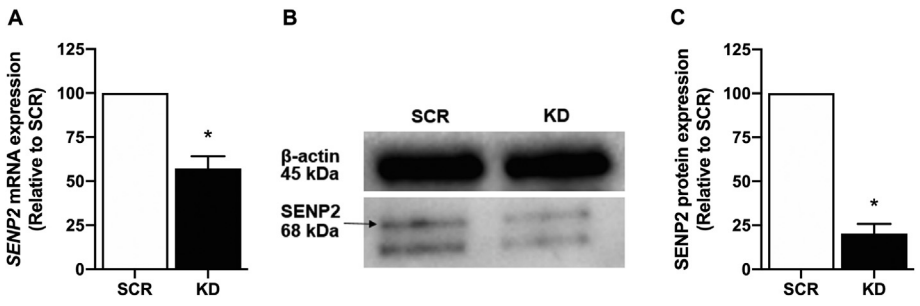

Fig. 2. Confirmation of SENP2-KD. Cells were harvested after seven days of differentiation. (**A**) RNA was harvested and expression of SUMO-specific peptidase 2 (SENP2) was analyzed by qPCR. Results are shown as mean ± SEM relative to the housekeeping gene ribosomal protein lateral stalk subunit P0 (*RPLP0*) and normalized to SCR cells, from six individual experiments ($n = 6$). (**B and C**) Protein expressions of SUMO-specific peptidase 2 (SENP2) and β-actin were analyzed by immunoblotting of protein isolated from cell lysates. A non-transduced cell sample was also included to ensure that the scrambled virus did not affect the cells; no differences were observed (data not shown). Binding of SENP2 occurs at about 68 kDa whereas β-actin binds at approximately 45 kDa. B, One representative immunoblot. C, Quantified immunoblot of three individual experiments ($n = 3$). *Statistically significant versus SCR cells ($p \leq 0.05$, paired *t*-test). SCR, control cells, i.e., scrambled vector; KD, knockdown cells, i.e., vector for SENP2 knockdown.

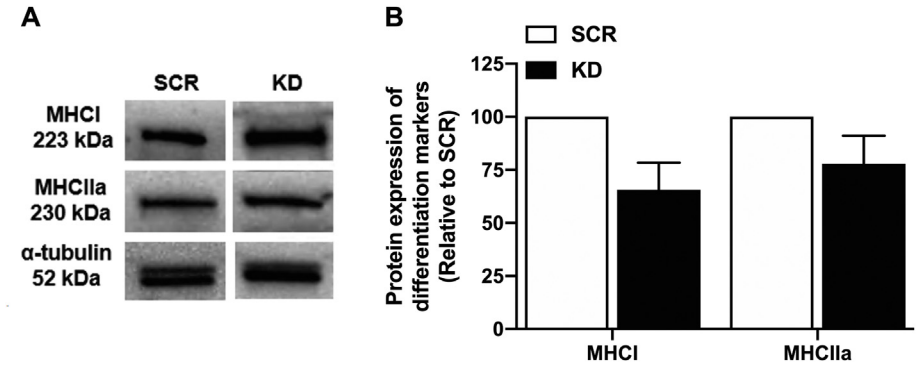

Fig. 3. Myotube differentiation was not affected SENP2-KD. Cells were harvested after seven days of differentiation. Protein expressions of the markers of differentiation myosin heavy chain (MHC) I and IIa and the housekeeping protein α-tubulin were analyzed by immunoblotting of protein isolated from cell lysates. Binding of MHCI occurs at about 223 kDa, MHCIIa at about 230 kDa, and α-tubulin at approximately 52 kDa. (**A**) One representative immunoblot. (**B**) Quantified immunoblot of three individual experiments ($n = 3$). SCR, control cells, i.e., scrambled vector; KD, knockdown cells, i.e., vector for SENP2 knockdown.

was lower in the SENP2-KD myotubes compared to control myotubes (Fig. 8D). In order to study the differences in basal glucose metabolism and the blunted insulin response in SENP2-KD myotubes further, we analyzed the mRNA expression of selected genes (Fig. 8E). mRNA expression of glucose transporter (*GLUT*) *1* and insulin receptor substrate (*IRS*) *1* was not different between SENP2-KD and control myotubes. There was a non-significant trend ($p = 0.09$) towards increased mRNA expression of pyruvate dehydrogenase kinase (*PDK*) *4* in the myotubes with downregulated SENP2.

4. Discussion

In this study, we demonstrate that SENP2-KD had a major impact on lipid metabolism, glucose metabolism and insulin-stimulated glycogen synthesis. SENP2-KD reduced acute (4 h incubation) oxidation of oleic acid and oxidative reserve capacity, incorporation of oleic acid into cellular lipids and promoted a higher oxidation of prelabeled (24 h incubation) oleic acid, whereas for glucose metabolism we observed an increased uptake of glucose and a blunted insulin-stimulated glycogen synthesis. This blunted effect of insulin was confirmed by a lack of insulin-stimulated Akt phosphorylation in SENP2-KD myotubes. In line with this, total Akt protein expression was lower in SENP2-KD myotubes.

Myotubes proliferate as myoblasts before they fuse into multinucleated myotubes. To establish if we could transduce the cells during proliferation, we needed to establish when expression of SENP2 was highest in the muscle cells and thus most likely important for myocyte function. Expression of SENP2 first started to increase after initiation of differentiation and continued to increase throughout differentiation. Therefore, we decided to transduce during proliferation. Visual examination in the microscope during cell proliferation and differentiation did not identify any morphological changes induced by SENP2-KD (data not shown). Protein expression of the differentiation markers MHCI and MHCIIa was not affected by SENP2-KD either. Combined these data suggests that SENP2-KD did not alter any major myocyte characteristics.

It has previously been shown that SENP2 is an important regulator of fatty acid metabolism in skeletal muscle of mice. Palmitic acid activated SENP2 in C2C12 myotubes and further increased expressions of genes involved in fatty acid oxidation (Do Koo et al., 2015). Treatment of our primary human myotubes with palmitic acid did not affect uptake or oxidation of oleic acid or mRNA expression of *SENP2* (data not shown). Furthermore, the previous work with murine cells showed that downregulation of SENP2 suppressed the palmitic acid-induced increase in gene expressions and thereby abolished fatty acid oxidation (Do Koo et al., 2015). We observed both a reduced fatty acid oxidation and reduced oxidative reserve capacity from acutely available oleic acid after SENP2-KD in human myotubes. After prelabeling the cells with oleic acid for 24 h, myotubes with and without SENP2-KD handled the oleic acid differently. Compared to control cells, SENP2-KD reduced the total incorporation of oleic acid into cellular lipids and the distribution of complex lipids changed in the myotubes: less was incorporated into TAG and relatively more into the other complex lipids (PL, DAG, FFA, and CE). FFA and DAG are intermediates for TAG synthesis at the same time as they are degradation products from lipolysis. DAG can be converted to either TAG or PL. Thus, it seems that SENP2-KD promoted PL synthesis to a greater extent than TAG synthesis. Increased proportion of intermediates in addition to reduced proportion of TAG may suggest an increased lipolysis after SENP2-KD in human myotubes. However, this needs to be further elucidated. Furthermore, in line with the reduced

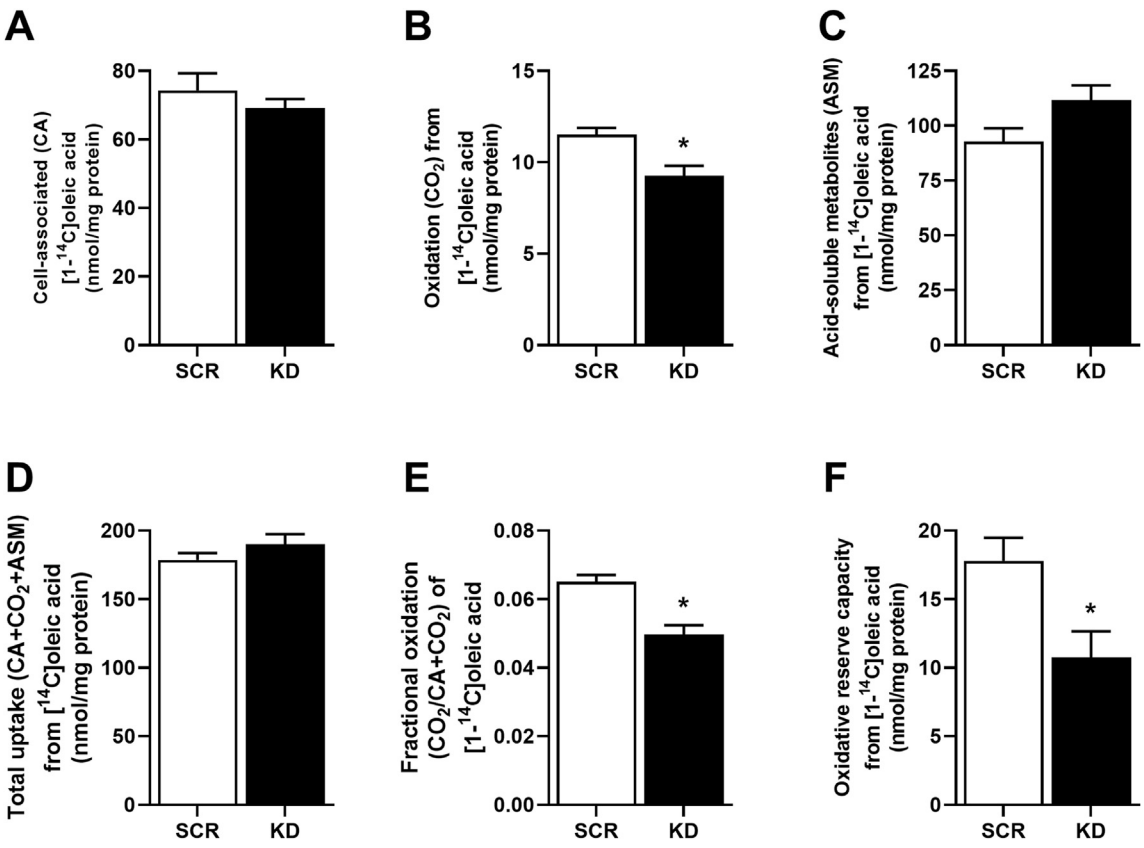

Fig. 4. Role of SENP2 for metabolism of fatty acids after acute incubation in human myotubes. Human myotubes were incubated with 100 μM [1-^{14}C]oleic acid (18.5 kBq/ml) for 4 h. Cell-associated (CA) radioactivity (**A**), complete oxidation measured as trapped CO_2 (**B**) and acid-soluble metabolites (ASM) (**C**) were analyzed. The combination of CA, CO_2 and ASM was taken as a measurement of total cellular oleic acid uptake (**D**). Fractional oleic acid oxidation was calculated as CO_2/CA + CO_2+ASM (**E**). As some parallel wells were treated with the mitochondrial uncoupler FCCP, oxidative reserve capacity was calculated as CO_2 from FCCP-treated cells − CO_2 from untreated cells (**F**). Results are shown as mean ± SEM in absolute values, nmol/mg protein from four individual experiments ($n = 4$) with eight replicates. *Statistically significant versus SCR cells ($p \leq 0.05$, mixed-model analysis). KD, cells with SENP2 knockdown; SCR, control cells i.e., with scrambled vector.

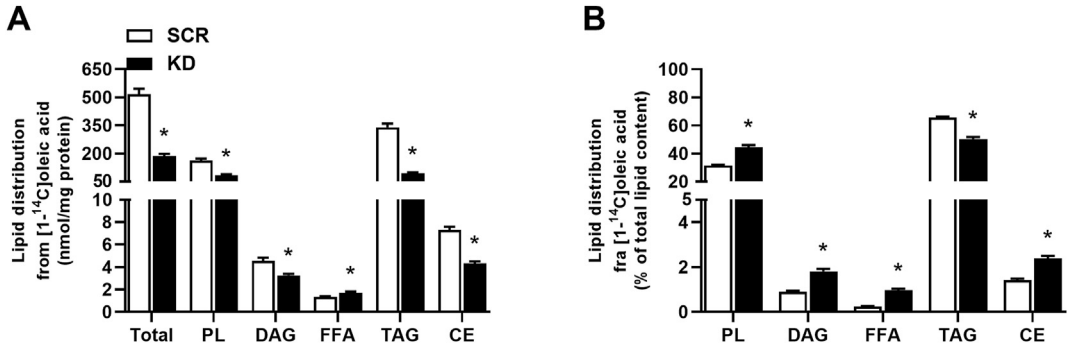

Fig. 5. Role of SENP2 for lipid distribution of oleic acid in human myotubes. Human myotubes were on day six of differentiation incubated with 100 μM [1-^{14}C] oleic acid (18.5 kBq/ml) for 24 h. Lipids were separated by thin layer chromatography and quantified by liquid scintillation. Results are shown as mean ± SEM for absolute values, nmol/mg protein (**A**) and related to total lipid content, % (**B**) from four individual experiments ($n = 4$) with three replicates. *Statistically significant versus SCR cells ($p \leq 0.05$, paired *t*-test). CE, cholesteryl ester; DAG, diacylglycerol; FFA, free fatty acids; KD, cells with SENP2 knockdown; PL, phospholipid; SCR, control cells i.e., with scrambled vector; TAG, triacylglycerol.

incorporation into lipids from prelabeled oleic acid in SENP2-KD myotubes, fatty acid oxidation was increased in these cells compared to control cells, both complete (measured as CO_2) and incomplete oxidation (measured as ASMs). This corresponds with recent findings from mice with liver-specific knockout of Senp2 where Senp2 deficiency upregulated genes involved in fatty acid oxidation and downregulated genes involved in lipogenesis (Liu et al., 2021). Further, it seems like the uptake of oleic acid, by looking at the sum of total oleic acid incorporation and total oxidized lipids (complete and incomplete), is somewhat lower (approximately 20%) in SENP2-KD cells compared to controls. This may explain some of the reduction in total lipid incorporation after SENP2-KD; however, as the relative increase in oxidation, particular incomplete oxidation (approximately 75%), is much higher than the apparent reduction in total uptake, we believe this to be the main reason behind the reduced total lipid incorporation.

SENP1 has previously been shown to link glucose metabolism to amplification of insulin secretion and demonstrate that restoration of this axis rescues β-cell function in T2DM (Ferdaoussi et al., 2015), whereas

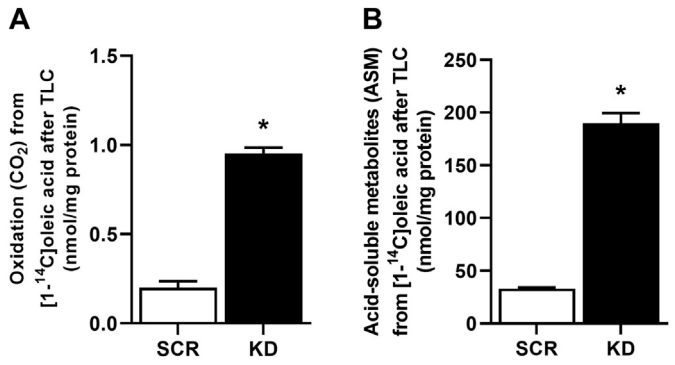

Fig. 6. Role of SENP2 in oxidation after prelabeling with oleic acid in human myotubes. Human myotubes were on day six of differentiation incubated with 100 μM [1-^{14}C]oleic acid (18.5 kBq/ml) for 24 h in order to measure distribution of oleic acid into complex lipids. Thereafter, the radiolabeled medium was saved and oxidation (CO_2) of oleic acid (**A**) and acid-soluble metabolites (ASM) from oleic acid (**B**) were measured. Results are shown as mean ± SEM in absolute values, nmol/mg protein, from four individual experiments ($n = 4$) with one (A) or three (B) replicates. *Statistically significant versus SCR cells ($p \leq 0.05$, paired *t*-test). KD, cells with SENP2 knockdown; SCR, control cells i.e., with scrambled vector; TLC, thin layer chromatography.

SENP2 has been suggested to play a role in enhancing β-cell mass in response to chronic high-glucose in pancreatic INS1-cells (Jung et al., 2016). Do Koo et al. observed that SENP2 overexpression in mice muscle alleviated HFD-induced obesity and insulin resistance, but it was unsure if these were direct SENP2 effects or secondary *in vivo* effects (Do Koo et al., 2015). In the cancerous MCF7 and MEF cells, it has been shown that SENP2 negatively regulated aerobic glycolysis. In MCF7 cells, overexpression of SENP2 led to reduced glucose uptake and production of lactate, inducing an increased ATP production (Tang et al., 2013). Furthermore, along with increased glucose oxidation, overexpression of SENP2 in both cell types caused reduced expression levels of key enzymes important for glycolysis indicating an inhibited glycolysis and increased oxidative phosphorylation. In contrast, knocking out SENP2 in MEF cells increased glucose uptake and lactate production but reduced ATP level (Tang et al., 2013). However, it is well known that metabolism in cancer cells is particular. Yet, the studies suggest that SENP2 might have a role in glucose metabolism, but the role of SENP2 in human skeletal muscle has not previously been examined. We observed that SENP2-KD in myotubes resulted in increased glucose uptake and an overall reduction in the proportion of glucose taken up that was oxidized (fractional oxidation). However, this was not explained by the expression of selected genes; neither mRNA expression of the basal glucose transporter, *GLUT1*, nor the metabolic regulator *PDK4* was significantly affected by down-regulation of SENP2.

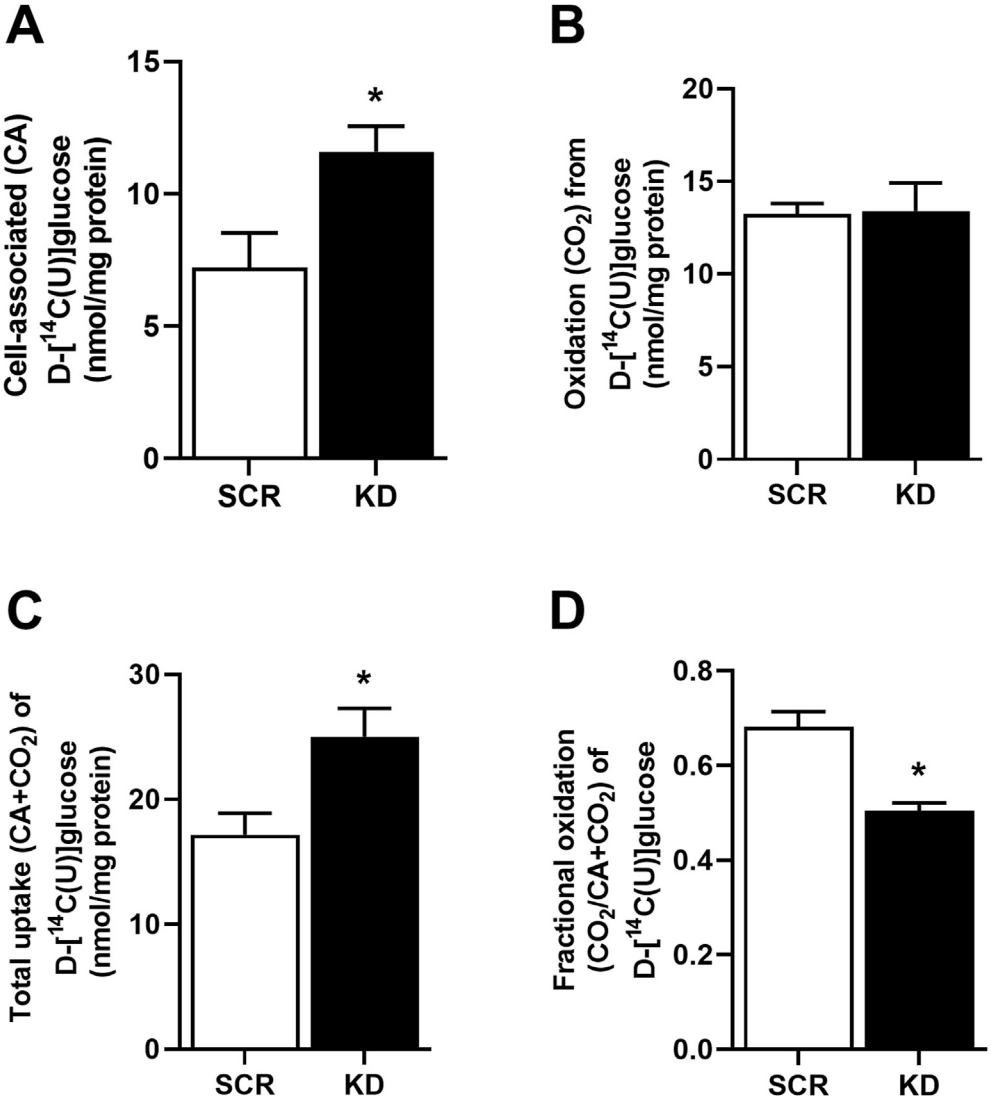

Fig. 7. Role of SENP2 for glucose metabolism in human myotubes. Human myotubes were incubated with 100 μM D-[^{14}C(U)]glucose (18.5 kBq/ml) for 4 h. Cell-associated (CA) radioactivity (**A**) and complete oxidation measured as trapped CO_2 (**B**) were analyzed. The combination of CA and CO_2 was taken as a measurement of total cellular glucose uptake (**C**). Fractional glucose oxidation was calculated as CO_2/CA + CO_2 (**D**). Results are shown as mean ± SEM in absolute values, nmol/mg protein from four individual experiments ($n = 4$) with eight replicates. *Statistically significant versus SCR cells ($p \leq 0.05$, mixed-model analysis). KD, cells with SENP2 knockdown; SCR, control cells i.e., with scrambled vector.

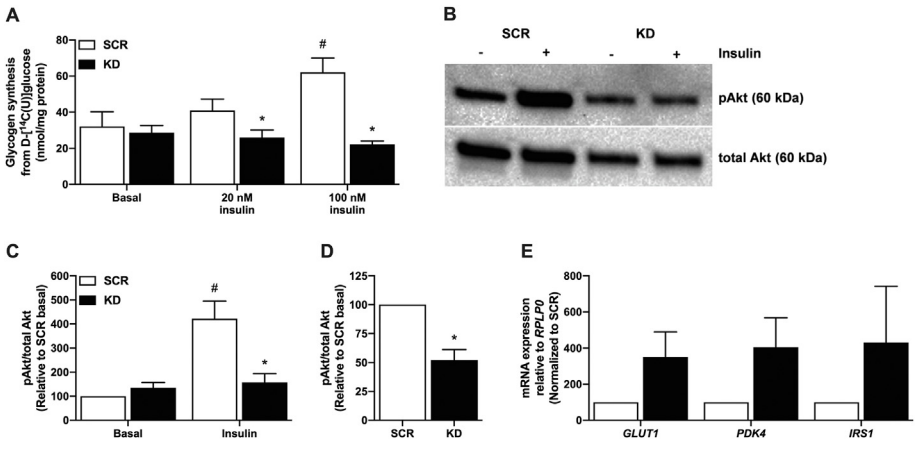

Fig. 8. Role of SENP2 for basal and insulin-stimulated glycogen synthesis and Akt phosphorylation in human myotubes. (**A**) Myotubes were starved for 1.5 h before incubated for 3 h with 5.5 mM D-[^{14}C(U)]glucose (37 kBq/ml) with no insulin (basal), 20 nM or 100 nM insulin. Results are shown as mean ± SEM in absolute values, nmol/mg protein, from four individual experiments ($n = 4$). (**B-D**) Akt phosphorylation and total Akt protein expression by immunoblotting. Myotubes were incubated for 15 min with 100 nM insulin before protein was isolated and the amount of total Akt and pAkt were assessed by immunoblotting. B, a representative immunoblot. C and D, quantified immunoblots relative to SCR. Results are shown as mean ± SEM from six individual experiments ($n = 6$). (**E**) mRNA expression of selected genes. RNA was harvested and expression of glucose transporter (*GLUT*) *1*, pyruvate dehydrogenase kinase (*PDK*) *4* and insulin receptor substrate (*IRS*) *1* were analyzed by qPCR. Results are shown as mean ± SEM relative to the housekeeping gene ribosomal protein lateral stalk subunit P0 (*RPLP0*) and normalized to SCR cells, from six individual experiments ($n = 6$). *Statistically significant versus SCR cells ($p \leq 0.05$, paired *t*-test). #Statistically significant versus to SCR basal ($p \leq 0.05$, paired *t*-test). KD, cells with SENP2 knockdown; SCR, control cells i.e., with scrambled vector.

Reduced amount of SENP2 is thought to lead to a reduced activation of PPARs (Do Koo et al., 2015). PPARs are targets for thiazolidinediones (glitazones) that are known to improve insulin sensitivity in subjects with T2DM. Thus, the question was whether SENP2-KD and consequently reduced PPAR activity would reduce insulin sensitivity in our myotubes. We observed a marked reduction in insulin-stimulated glycogen synthesis in knockdown myotubes, accompanied by a blunted insulin-stimulated phosphorylation of Akt, showing clearly that SENP2 is important for insulin sensitivity in human skeletal muscle cells. Increased insulin-stimulated glycogen synthesis may be a result of the increased glucose uptake that insulin stimulated directly or through its effect on glycogen synthase (Lawrence and Roach, 1997). A previous study in L6 cells indicated that SUMOylation could lead to upregulation of GLUT4 (Giorgino et al., 2000). However, a recent study by Carmichael et al. contradicts the hypothesis of SUMOylation increasing GLUT4-mediated glucose uptake as SUMOylation did not affect insulin-dependent GLUT4 trafficking in L6 myocytes (Carmichael et al., 2019). The ratio of GLUT1 to GLUT4 is higher in human myotubes compared to adult muscle (Sarabia et al., 1992), resulting in lower insulin responsiveness of glucose transport (Sarabia et al., 1992; Al-Khalili et al., 2003). However, the molecular mechanisms of glucose transport remain the same (Al-Khalili et al., 2003). mRNA expression of *GLUT1* and *IRS1* was not different between control myotubes and SENP2-KD myotubes. Based on the results of Do Koo et al. on lipid metabolism, decreased deSUMOylation of PPAR (i.e., reduced PPAR activity) is hypothesized to be behind the found effect of SENP2 knockdown. A weakness of the present study is the lack of examination of PPAR SUMOylation. However, another target of SUMOylation include Akt itself (De la Cruz-Herrera et al., 2015). Examining total protein expression of Akt, SENP2-KD cells had significantly lower expression than control cells. Furthermore, previous data shows that although PPARγ is low expressed in muscle cells, PPARγ knockdown resulted in reduced insulin sensitivity in C2C12-cells (Verma et al., 2004). Hence, it seems likely that the SENP2 effect observed is secondary to reduced PPAR activity.

The results from the present study are somewhat contradictory to the findings by Do Koo et al. (Do Koo et al., 2015). Do Koo et al. examined the role of SENP2 in murine cells. Even though rodents have similarities to humans on several metabolic characteristics, metabolism of the two species are not identical. Due to smaller body weight, rodents have a higher basal metabolic rate, and main glucose uptake occurs in the liver of rodents but in skeletal muscle of humans. Therefore, direct transfer of findings from rodents to humans must be performed with caution (Kleinert et al., 2018). This may explain the different observations in lipid metabolism between our two studies, as well as different methodologies for the transgenic studies.

In conclusion, this work shows for the first time that SENP2 exerts a critical role for both glucose and lipid metabolism in human myotubes. Interestingly, both insulin-stimulated glycogen synthesis and Akt phosphorylation were blunted in SENP2-KD myotubes. Future studies should examine the role of SENP2 in regulation of insulin sensitivity, highlighting the potential of SENP2 as a novel target in the combat against the ever-increasing obesity and diabetes pandemic.

CRediT authorship contribution statement

Jenny Lund: Conceptualization, Methodology, Investigation, Formal analysis, Visualization, Validation, Project administration, Supervision, Writing – original draft, Writing – review & editing. **Solveig A. Krapf:** Conceptualization, Methodology, Investigation, Formal analysis, Validation, Writing – original draft, Writing – review & editing. **Medina Sistek:** Investigation, Writing – review & editing. **Hege G. Bakke:** Methodology, Investigation, Writing – review & editing. **Stefano Bartesaghi:** Conceptualization, Methodology, Writing – review & editing. **Xiao-Rong Peng:** Conceptualization, Methodology, Writing – review & editing. **Arild C. Rustan:** Methodology, Funding acquisition, Resources, Writing – review & editing. **G. Hege Thoresen:** Conceptualization, Methodology, Funding acquisition, Resources, Writing – review & editing. **Eili T. Kase:** Conceptualization, Methodology, Validation, Project administration, Funding acquisition, Resources, Supervision, Writing – original draft, Writing – review & editing.

Declaration of competing interest

The authors declare that they have no known competing financial interests or personal relationships that could have appeared to influence the work reported in this paper.

Acknowledgements

The authors would like to acknowledge Eva Töppner Carlsson, Simonetta Wallin and Matthew Harms for excellent technical assistance at AstraZeneca.

Appendix A. Supplementary data

Supplementary data to this article can be found online at https://doi.org/10.1016/j.crphar.2021.100061.

Funding

This work was solely funded by the University of Oslo.

References

Aas, V., Kase, E., Solberg, R., Jensen, J., Rustan, A., 2004. Chronic hyperglycaemia promotes lipogenesis and triacylglycerol accumulation in human skeletal muscle cells. Diabetologia 47, 1452–1461.

Aas, V., Rokling-Andersen, M., Wensaas, A., Thoresen, G., Kase, E., Rustan, A., 2005. Lipid metabolism in human skeletal muscle cells: effects of palmitate and chronic hyperglycaemia. Acta Physiol. Scand. 183, 31–41.

Aas, V., Rokling-Andersen, M.H., Kase, E.T., Thoresen, G.H., Rustan, A.C., 2006. Eicosapentaenoic acid (20: 5 n-3) increases fatty acid and glucose uptake in cultured human skeletal muscle cells. J. Lipid Res. 47, 366–374.

Aas, V., Hessvik, N.P., Wettergreen, M., Hvammen, A.W., Hallén, S., Thoresen, G.H., Rustan, A.C., 2011. Chronic hyperglycemia reduces substrate oxidation and impairs metabolic switching of human myotubes. BBA Mol. Basis Dis. 1812, 94–105.

Al-Khalili, L., Chibalin, A., Kannisto, K., Zhang, B., Permert, J., Holman, G., Ehrenborg, E., Ding, V., Zierath, J., Krook, A., 2003. Insulin action in cultured human skeletal muscle cells during differentiation: assessment of cell surface GLUT4 and GLUT1 content. Cell. Mol. Life Sci. 60, 991–998.

Bakke, S.S., Moro, C., Nikolić, N., Hessvik, N.P., Badin, P.-M., Lauvhaug, L., Fredriksson, K., Hesselink, M.K., Boekschoten, M.V., Kersten, S., 2012. Palmitic acid follows a different metabolic pathway than oleic acid in human skeletal muscle cells; lower lipolysis rate despite an increased level of adipose triglyceride lipase. BBA Mol. Cell Biol. Lipids. 1821, 1323–1333.

Barde, I., Salmon, P., Trono, D., 2010. Production and titration of lentiviral vectors. Curr. Protoc. Neurosci. 53, 4.21. 21-24.21. 23.

Békés, M., Prudden, J., Srikumar, T., Raught, B., Boddy, M.N., Salvesen, G.S., 2011. The dynamics and mechanism of SUMO chain deconjugation by SUMO-specific proteases. J. Biol. Chem. 286, 10238–10247.

Boren, J., Taskinen, M.R., Olofsson, S.O., Levin, M., 2013. Ectopic lipid storage and insulin resistance: a harmful relationship. J. Intern. Med. 274, 25–40.

Bruce, C.R., Hoy, A.J., Turner, N., Watt, M.J., Allen, T.L., Carpenter, K., Cooney, G.J., Febbraio, M.A., Kraegen, E.W., 2009. Overexpression of carnitine palmitoyltransferase-1 in skeletal muscle is sufficient to enhance fatty acid oxidation and improve high-fat diet–induced insulin resistance. Diabetes 58, 550–558.

Carmichael, R.E., Wilkinson, K.A., Craig, T.J., 2019. Insulin-dependent GLUT4 trafficking is not regulated by protein SUMOylation in L6 myocytes. Sci. Rep. 9, 1–9.

Choi, C.S., Savage, D.B., Abu-Elheiga, L., Liu, Z.-X., Kim, S., Kulkarni, A., Distefano, A., Hwang, Y.-J., Reznick, R.M., Codella, R., 2007. Continuous fat oxidation in acetyl–CoA carboxylase 2 knockout mice increases total energy expenditure, reduces fat mass, and improves insulin sensitivity. Proc. Natl. Acad. Sci. U.S.A 104, 16480–16485.

Chung, S.S., Ahn, B.Y., Kim, M., Choi, H.H., Park, H.S., Kang, S., Park, S.G., Kim, Y.-B., Cho, Y.M., Lee, H.K., 2010. Control of adipogenesis by the SUMO-specific protease SENP2. Mol. Cell Biol. 30, 2135–2146.

Chung, S.S., Ahn, B.Y., Kim, M., Kho, J.H., Jung, H.S., Park, K.S., 2011. SUMO modification selectively regulates transcriptional activity of peroxisome-proliferator-activated receptor γ in C2C12 myotubes. Biochem. J. 433, 155–161.

Corpeleijn, E., Hessvik, N.P., Bakke, S.S., Levin, K., Blaak, E.E., Thoresen, G.H., Gaster, M., Rustan, A.C., 2010. Oxidation of intramyocellular lipids is dependent on mitochondrial function and the availability of extracellular fatty acids. Am. J. Physiol. Endocrinol. Metab. 299, E14–E22.

De la Cruz-Herrera, C., Campagna, M., Lang, V., del Carmen González-Santamaría, J., Marcos-Villar, L., Rodríguez, M., Vidal, A., Collado, M., Rivas, C., 2015. SUMOylation regulates AKT1 activity. Oncogene 34, 1442–1450.

Czech, M.P., 2017. Insulin action and resistance in obesity and type 2 diabetes. Nat. Med. 23, 804.

Desvergne, B., Wahli, W., 1999. Peroxisome proliferator-activated receptors: nuclear control of metabolism. Endocr. Rev. 20, 649–688.

Feige, J.N., Lagouge, M., Canto, C., Strehle, A., Houten, S.M., Milne, J.C., Lambert, P.D., Mataki, C., Elliott, P.J., Auwerx, J., 2008. Specific SIRT1 activation mimics low energy levels and protects against diet-induced metabolic disorders by enhancing fat oxidation. Cell Metabol. 8, 347–358.

Ferdaoussi, M., Dai, X., Jensen, M.V., Wang, R., Peterson, B.S., Huang, C., Ilkayeva, O., Smith, N., Miller, N., Hajmrle, C., 2015. Isocitrate-to-SENP1 signaling amplifies insulin secretion and rescues dysfunctional β cells. J. Clin. Invest. 125, 3847–3860.

Gaster, M., Rustan, A.C., Aas, V., Beck-Nielsen, H., 2004. Reduced lipid oxidation in skeletal muscle from type 2 diabetic subjects may be of genetic origin: evidence from cultured myotubes. Diabetes 53, 542–548.

Giorgino, F., De Robertis, O., Laviola, L., Montrone, C., Perrini, S., McCowen, K.C., Smith, R.J., 2000. The sentrin-conjugating enzyme mUbc9 interacts with GLUT4 and GLUT1 glucose transporters and regulates transporter levels in skeletal muscle cells. Proc. Natl. Acad. Sci. U.S.A 97, 1125–1130.

Hay, R.T., 2005. SUMO: a history of modification. Mol. Cell. 18, 1–12.

Hessvik, N.P., Bakke, S.S., Fredriksson, K., Boekschoten, M.V., Fj, A., Koster, G., Hesselink, M.K., Kersten, S., Kase, E.T., Rustan, A.C., 2010. Metabolic switching of human myotubes is improved by n-3 fatty acids. J. Lipid Res. 51, 2090–2104.

Holloway, G.P., 2009. Mitochondrial function and dysfunction in exercise and insulin resistance. Appl. Physiol. Nutr. Metabol. 34, 440–446.

Huang, C., Han, Y., Wang, Y., Sun, X., Yan, S., Yeh, E.T., Chen, Y., Cang, H., Li, H., Shi, G., 2009. SENP3 is responsible for HIF-1 transactivation under mild oxidative stress via p300 de-SUMOylation. EMBO J. 28, 2748–2762.

Jung, H.S., Kang, Y.M., Park, H.S., Ahn, B.Y., Lee, H., Kim, M.J., Jang, J.Y., Kim, S.-W., 2016. Senp2 expression was induced by chronic glucose stimulation in INS1 cells, and it was required for the associated induction of Ccnd1 and Mafa. Islets 8, 207–216.

Kase, E.T., Wensaas, A.J., Aas, V., Højlund, K., Levin, K., Thoresen, G.H., Beck-Nielsen, H., Rustan, A.C., Gaster, M., 2005. Skeletal muscle lipid accumulation in type 2 diabetes may involve the liver X receptor pathway. Diabetes 54, 1108–1115.

Kase, E.T., Feng, Y.Z., Badin, P.-M., Bakke, S.S., Laurens, C., Coue, M., Langin, D., Gaster, M., Thoresen, G.H., Rustan, A.C., 2015. Primary defects in lipolysis and insulin action in skeletal muscle cells from type 2 diabetic individuals. BBA Mol. Cell Biol. Lipids 1851, 1194–1201.

Kelley, D.E., Goodpaster, B.H., 2001. Skeletal muscle triglyceride. An aspect of regional adiposity and insulin resistance. Clin. Diabetol. 2, 255–266.

Kleinert, M., Clemmensen, C., Hofmann, S.M., Moore, M.C., Renner, S., Woods, S.C., Huypens, P., Beckers, J., De Angelis, M.H., Schürmann, A., 2018. Animal models of obesity and diabetes mellitus. Nat. Rev. Endocrinol. 14, 140.

Do Koo, Y., Choi, J.W., Kim, M., Chae, S., Ahn, B.Y., Kim, M., Oh, B.C., Hwang, D., Seol, J.H., Kim, Y.-B., 2015. SUMO-specific protease 2 (SENP2) is an important regulator of fatty acid metabolism in skeletal muscle. Diabetes 64, 2420–2431.

Do Koo, Y., Lee, J.S., Lee, S.-A., Quaresma, P.G., Bhat, R., Haynes, W.G., Park, Y.J., Kim, Y.-B., Chung, S.S., Park, K.S., 2019. SUMO-specific protease 2 mediates leptin-induced fatty acid oxidation in skeletal muscle. Metabolism 95, 27–35.

Lawrence, J.C., Roach, P.J., 1997. New insights into the role and mechanism of glycogen synthase activation by insulin. Diabetes 46, 541–547.

Liu, Y., Dou, X., Zhou, W.y., Ding, M., Liu, L., Du, R.q., Guo, L., Qian, S.w., Tang, Y., Yang, Q.q., 2021. Hepatic SENP2 controls systemic metabolism via SUMOylation-dependent regulation of liver-adipose tissue crosstalk. Hepatology 74, 1864–1883.

Lund, J., Rustan, A.C., Løvsletten, N.G., Mudry, J.M., Langleite, T.M., Feng, Y.Z., Stensrud, C., Brubak, M.G., Drevon, C.A., Birkeland, K.I., 2017. Exercise in vivo marks human myotubes in vitro: training-induced increase in lipid metabolism. PloS One 12, e0175441.

Martins, A.R., Nachbar, R.T., Gorjao, R., Vinolo, M.A., Festuccia, W.T., Lambertucci, R.H., Cury-Boaventura, M.F., Silveira, L.R., Curi, R., Hirabara, S.M., 2012. Mechanisms underlying skeletal muscle insulin resistance induced by fatty acids: importance of the mitochondrial function. Lipids Health Dis. 11, 1–11.

Mikolajczyk, J., Drag, M., Békés, M., Cao, J.T., Ronai, Z.e., Salvesen, G.S., 2007. Small ubiquitin-related modifier (SUMO)-specific proteases: profiling the specificities and activities of human SENPs. J. Biol. Chem. 282, 26217–26224.

Nayak, A., Müller, S., 2014. SUMO-specific proteases/isopeptidases: SENPs and beyond. Genome Biol. 15, 1–7.

Perdomo, G., Commerford, S.R., Richard, A.-M.T., Adams, S.H., Corkey, B.E., O'Doherty, R.M., Brown, N.F., 2004. Increased β-oxidation in muscle cells enhances insulin-stimulated glucose metabolism and protects against fatty acid-induced insulin resistance despite intramyocellular lipid accumulation. J. Biol. Chem. 279, 27177–27186.

Perreault, L., Newsom, S., Strauss, A., Kerege, A., Kahn, D., Harrison, K., Snell-Bergeon, J., Nemkov, T., D'Alessandro, A., Jackman, M., 2018. Intracellular localization of diacylglycerols and sphingolipids influences insulin sensitivity and mitochondrial function in human skeletal muscle. JCI Insight 3, 1–21.

Petersen, K.F., Shulman, G.I., 2006. Etiology of insulin resistance. Am. J. Med. 119, S10–S16.

Petersen, M.C., Shulman, G.I., 2018. Mechanisms of insulin action and insulin resistance. Physiol. Rev. 98, 2133–2223.

Reverter, D., Lima, C.D., 2006. Structural basis for SENP2 protease interactions with SUMO precursors and conjugated substrates. Nat. Struct. Biol. 13, 1060–1068.

Rytinki, M.M., Palvimo, J.J., 2009. SUMOylation attenuates the function of PGC-1α. J. Biol. Chem. 284, 26184–26193.

Sarabia, V., Lam, L., Burdett, E., Leiter, L., Klip, A., 1992. Glucose transport in human skeletal muscle cells in culture. Stimulation by insulin and metformin. J. Clin. Invest. 90, 1386–1395.

Skrede, S., Bremer, J., Berge, R., Rustan, A., 1994. Stimulation of fatty acid oxidation by a 3-thia fatty acid reduces triacylglycerol secretion in cultured rat hepatocytes. J. Lipid Res. 35, 1395–1404.

Sugden, M., Holness, M., 2006. Skeletal muscle lipid metabolism and the adipomuscular axis. Future Lipidol. 1, 153–163.

Tang, S., Huang, G., Tong, X., Xu, L., Cai, R., Li, J., Zhou, X., Song, S., Huang, C., Cheng, J., 2013. Role of SUMO-specific protease 2 in reprogramming cellular glucose metabolism. PloS One 8, e63965.

Tomás, E., Lin, Y.S., Dagher, Z., Saha, A., Luo, Z., Ido, Y., Ruderman, N.B., 2002. Hyperglycemia and insulin resistance: possible mechanisms. Ann. N. Y. Acad. Sci. 967, 43–51.

Verma, N.K., Singh, J., Dey, C.S., 2004. PPAR-γ expression modulates insulin sensitivity in C2C12 skeletal muscle cells. Br. J. Pharmacol. 143, 1006–1013.

Wensaas, A., Rustan, A., Lövstedt, K., Kull, B., Wikström, S., Drevon, C., Hallen, S., 2007. Cell-based multiwell assays for the detection of substrate accumulation and oxidation. J. Lipid Res. 48, 961–967.

Yamashita, D., Yamaguchi, T., Shimizu, M., Nakata, N., Hirose, F., Osumi, T., 2004. The transactivating function of peroxisome proliferator-activated receptor γ is negatively regulated by SUMO conjugation in the amino-terminal domain. Gene Cell. 9, 1017–1029.